

1 **Autoantibody-Driven Monocyte Dysfunction in Post-COVID Syndrome with Myalgic**
2 **Encephalomyelitis/Chronic Fatigue Syndrome**

3
4 Alexander Hackel^{1#*} and Franziska Sotzny^{#2}, Elise Mennenga¹, Harald Heidecke³,
5 Kai Schulze-Foster³, Konstantinos Furlakis¹, Susanne Lüders¹,
6 Hanna Grasshoff¹, Kerstin Rubarth^{4‡}, Frank Konietschke⁴, Tanja Lange¹,
7 Carmen Scheibenbogen², Reza Akbarzadeh^{1‡}, Gabriela Riemekasten^{1‡}

8
9 ¹Department of Rheumatology and Clinical Immunology, University of Lübeck, Lübeck,
10 Germany

11 ²Institute for Medical Immunology, Charité–Universitätsmedizin Berlin, Berlin, Germany
12 Corporate Member of Freie Universität Berlin and Humboldt Universität Zu Berlin, Berlin,
13 Germany

14 ³CellTrend GmbH, Luckenwalde, Germany

15 ⁴Institute for Biometry and Clinical Epidemiology, Charite–Universitätsmedizin Berlin, Berlin,
16 German

17
18 *Corresponding author

19 ‡ Senior author

20 # Shared first author

21
22 **Correspondance:**

23 Dr. Alexander Hackel

24 Department of Rheumatology and Clinical Immunology, University of Lübeck

25 Address: Ratzeburger Allee 160, 23538 Lübeck

26 Telephone: +49 0451 500 45201

27 Email: alexandermaximilian.hackel@uksh.de

28
29 **Keywords:** Autoantibodies, Post-COVID Syndrom, ME/CFS, Monocyte-Derived Cytokines,
30 Biomarker

31
32 **Running title:** IgG-induced cytokine response of monocytes in PCS

33 **Abstract**

34 Post-COVID syndrome (PCS) has emerged as a significant health concern with persisting
35 symptoms. A subset of PCS patients develops severe myalgic encephalomyelitis/chronic
36 fatigue syndrome (pcME/CFS). Dysregulated autoantibodies (AABs) have been implicated in
37 PCS, contributing to immune dysregulation, impairment of autonomous nerve and vascular
38 function. As recently shown in autoimmune diseases, IgG fractions translate disease-specific
39 pathways into various cells. Therefore, we asked whether IgG fractions from PCS patients
40 could be applied in-vitro to identify specific cytokine responses for PCS patients without (nPCS)
41 and with pcME/CSF. To assess this, we have stimulated monocyte cell lines with IgG fractions
42 from PCS patients. Our findings reveal distinct cytokine responses induced by patient derived
43 AABs which are suggested in vascular and immune dysfunction. In contrast to nPCS,
44 pcME/CSF AABs induced enhanced neurotrophic responses, characterized by significant
45 cytokine correlations involving brain-derived neurotrophic factor (BDNF), glial cell-derived
46 neurotrophic factor (GDNF) and tumor necrosis factor superfamily member 14 (LIGHT).
47 Further, AAB-induced cytokine levels correlate with clinical symptoms. This study emphasizes
48 a contribution of AABs in PCS, in mitigating long-term immune dysregulation, and a need for
49 therapies modulating IgG-induced signaling pathways.

50 **Introduction**

51 Post-COVID syndrome (PCS) has become a major public health concern, affecting 10–20%
52 of individuals after SARS-CoV-2 infection. Symptoms persist for a minimum of two months and
53 often severely impair daily functioning. [1-3] Among these patients, a subgroup fulfills the
54 Canadian Consensus Criteria (CCC) for diagnosis of myalgic encephalomyelitis/chronic
55 fatigue syndrome (ME/CFS) [4-6]. The clinical overlap between PCS and ME/CFS highlights
56 the shared but poorly understood mechanisms underlying these conditions. Emerging
57 evidence implicates a complex interplay of immune dysregulation, endothelial dysfunction, and
58 vascular anomalies in PCS, which may differ from these in pcME/CFS [7-9]. Functional
59 autoantibodies (AABs) have been identified as significant contributors to immune dysregulation
60 in both acute and post-viral syndromes [10]. For example, AABs against renin-angiotensin
61 system (RAS)-related proteins, including angiotensin-converting enzyme 2 (ACE2) and
62 angiotensin type-1 receptor (AT1R), correlate with disease severity in acute COVID-19 and
63 vascular dysfunction in PCS [11]. Our studies suggest a contribution of specific AABs in
64 inflammatory conditions. As an example, AT1R AABs induced skin and lung inflammation as
65 well as endothelial apoptosis [12, 13]. In ME/CFS, disease-specific alterations in the G-protein
66 coupled receptor (GPCR) AAB network have been associated with key symptoms such as
67 fatigue, muscle pain, and neurocognitive impairments [14, 15]. Similar disruptions in PCS
68 suggest a shared mechanism of immune-mediated dysfunction, with GPCR AABs potentially
69 modulating both inflammatory and neurotrophic pathogenic alterations. Intriguingly, in PCS,
70 AABs against adrenergic receptors were identified as key markers distinguishing symptom
71 severity, emphasizing their contribution to vascular dysfunction and endothelial impairment
72 [16]. Similarly, in PCS, AABs targeting vasoregulatory and immune-modulatory proteins have
73 been linked to chronic vascular inflammation and immune dysregulation.

74 Monocytes, as pivotal responders of innate immunity, are emerging as key mediators in the
75 immunopathogenesis of PCS and pcME/CFS. In viral infections, monocytes act as first-line
76 effectors, contributing to immune defense and tissue repair. However, their dysregulation can
77 lead to pathological inflammation and tissue damage, as seen in macrophage activation
78 syndrome during severe COVID-19 [17, 18]. Monocyte-driven responses, particularly through
79 secreted cytokines such as CCL18, are also implicated in fibrotic and neurodegenerative
80 processes characteristic for autoimmune diseases such as systemic sclerosis, but also for
81 PCS [19]. As shown by our group, IgG fractions from patients with autoimmune diseases
82 induce a disease-specific protein pattern and pathways in monocytes [12]. The IgG-induced
83 secretome could thus serve as a biomarker for pathways present in their corresponding donor
84 and as a diagnostic tool. To address this hypothesis, the current study investigates the role of
85 AAB-induced monocyte activation in PCS and pcME/CFS. By focusing on the monocyte
86 secretome, this research aims to elucidate whether known mechanisms in ME/CFS such as

87 inflammatory and neurodegenerative processes are induced by AABs, whether IgG-induced
88 cytokines and proteins show associations with clinical findings, and whether the cytokine
89 signature could be used as diagnostic tool. Our study represents the first comprehensive
90 investigation into the interaction between AABs, monocyte activation, and disease
91 pathophysiology in PCS and pcME/CFS, offering new insights into potential therapeutic
92 targets.

93 **Methods**

94 **Cohort characteristics**

95 Female participants between 24 and 51 years were recruited at the Charité Fatigue Centre,
 96 Berlin. Serum samples were collected from 24 PCS patients with persistent fatigue and
 97 exercise intolerance following mild to moderate acute SARS-CoV-2 infection and from 12
 98 age-matched healthy controls (HCs). 12 out of 24 PCS patients fulfilled the Canadian
 99 Consensus Criteria (CCC) for diagnosis of ME/CFS (pcME/CFS), others were categorized as
 100 PCS none ME/CFS (nPCS), the PCS group includes both defined Subgroups. Most patients
 101 had a disease duration >6 months, in two of 11 pcME/CFS patients, and in two of 13 PCS
 102 patients with a disease duration < 6 months, the diagnosis was confirmed at month 6.
 103 Detailed cohort information is displayed in **Table 1**. Disease and symptom severity were
 104 assessed by questionnaires: The functional disability was evaluated by Bell score, ranging
 105 from 0 to 100 (with 100 for no restrictions) [20]. PEM severity was evaluated according to Cotler
 106 et al., with scores ranging from 0 to 46 (no to frequent/severe PEM) [21]. The severity of the
 107 key symptoms, fatigue, pain, and cognitive impairment was quantified using a Likert scale
 108 (1 = no symptoms to 10 = severe symptoms). Fatigue was additionally evaluated using the
 109 Chalder Fatigue Scale from 0 to 33 (no to heavy fatigue) [22]. Autonomic dysfunction was
 110 assessed using the Composite Autonomic Symptom Score 31 (COMPASS-31), ranging from
 111 0 to 100 (no to strongest impairment) [23]. Clinical data was collected and managed using
 112 REDCap electronic data capture tools hosted at Charité University Medicine Berlin [24, 25].
 113 Whole blood samples from participants were allowed to clot at room temperature and then
 114 centrifuged at 2000 x g for 15 min at 4°C. The purified serum was stored at -80°C for further
 115 analysis. SARS-CoV-2 Serology was performed at the Institute for Immunology at Charité
 116 Universitätsmedizin Berlin using Anti-SARS-CoV-2 ELISA (IgG) according to manufacturer
 117 protocol (Euroimmun Medizinische Labordiagnostika AG, Lübeck, Germany). This study was
 118 approved by the Ethics Committee of Charité Universitätsmedizin Berlin
 119 (EA2/067/20, EA2/066/20). The participants gave written informed consent.

120 **Table 1:** Clinical scorings and cohort characterization. Continuous variables were expressed
 121 as median and range. Univariate comparisons of study groups were done using the Kruskal–
 122 Wallis test (three groups) or the Mann-Whitney-U-Test (two groups). A two-tailed p-value of
 123 <0.05 was considered statistically significant. [n. a. = not assessed].

Cohort characterization	HC ¹	nPCS ¹	pcME/CFS ¹	p-value ²
Age [in years]	37 (24 - 51), n = 12	36 (27 - 50), n = 13	36 (28 - 51), n = 11	0.897
BMI	20.2 (20.2 - 20.2), n = 1	23.1 (18.4 - 34.8), n = 12	25.3 (15.4 - 40.8), n = 11	0.513
disease duration [years]	0.50 (0.35 - 0.88), n = 12	0.56 (0.36 - 1.03), n = 13	0.64 (0.42 - 1.99), n = 11	0.306
disease duration [months]	6.0 (4.2 - 10.6), n = 12	6.7 (4.4 - 12.4), n = 13	7.7 (5.1 - 23.9), n = 11	0.252

anti-NCAP-IgG	0.42 (0.00 - 1.44), n = 4	0.00 (0.00 - 3.99), n = 4	0.00 (0.00 - 7.36), n = 7	0.819
anti-Spike-IgG	3.9 (1.3 - 12.5), n = 12	5.8 (1.3 - 12.5), n = 12	6.7 (1.2 - 11.6), n = 9	>0.999
Cohort characterization				
Age [in years]	37 (24 - 51), n = 12	36 (27 - 50), n = 13	36 (28 - 51), n = 11	0.897
Clinical scorings	HC¹	nPCS¹	pcME/CFS¹	p-value²
Bell	N/A	50 (30 - 80), n = 13	30 (20 - 50), n = 11	0.012
PEM score	N/A	24.0 (21.0 - 32.0), n = 11	33.0 (25.0 - 44.0), n = 11	0.010
Role limitations due to physical health	N/A	0 (0 - 75), n = 13	0 (0 - 0), n = 11	0.027
Energy Fatigue	N/A	35 (5 - 55), n = 13	10 (0 - 55), n = 11	0.054
Emotional Wellbeing	N/A	68 (24 - 88), n = 13	64 (44 - 84), n = 11	0.930
Social Functioning	N/A	50 (12 - 100), n = 13	25 (0 - 75), n = 10	0.109
Pain	N/A	45 (10 - 78), n = 13	32 (0 - 55), n = 10	0.060
General health	N/A	38 (20 - 65), n = 12	30 (5 - 40), n = 11	0.045
Health Change	N/A	0 (0 - 25), n = 12	0 (0 - 75), n = 11	0.417
Physical Sum Scale	N/A	35 (25 - 43), n = 12	27 (10 - 34), n = 10	0.007
Psychical Sum Scale	N/A	38 (13 - 47), n = 12	31 (20 - 53), n = 10	0.722
Fatigue SY-1	N/A	6.00 (2.00 - 10.00), n = 13	8.00 (5.00 - 10.00), n = 11	0.088
Severity of Muscle Pain SY-6	N/A	5.00 (1.00 - 8.00), n = 13	7.00 (1.00 - 10.00), n = 11	0.519
Severity of Headache SY-7	N/A	6.50 (1.00 - 9.00), n = 12	4.00 (1.00 - 9.00), n = 11	0.106
Joint Paint SY-8	N/A	3.50 (1.00 - 8.00), n = 12	3.00 (1.00 - 10.00), n = 11	0.901
Fatigue Score	N/A	7.00 (2.25 - 8.50), n = 13	8.25 (5.25 - 10.00), n = 11	0.027
Cognitive Score	N/A	6.17 (1.67 - 7.67), n = 12	5.67 (3.00 - 7.00), n = 11	0.459
Immune Score	N/A	3.33 (1.00 - 8.00), n = 12	3.33 (1.67 - 7.67), n = 11	0.688
COMPASS-31 (total)	N/A	36 (2 - 51), n = 13	34 (10 - 70), n = 11	>0.999
-orthostatism	N/A	16 (0 - 32), n = 13	16 (0 - 40), n = 11	0.883
-vasomotor	N/A	0.00 (0.00 - 0.00), n = 13	0.00 (0.00 - 4.17), n = 11	0.023
-secremotor	N/A	6.4 (0.0 - 10.7), n = 13	4.3 (0.0 - 12.9), n = 11	>0.999
-gastrointestinal	N/A	6.2 (0.0 - 15.2), n = 13	7.1 (0.0 - 14.3), n = 11	0.954
-bladder	N/A	1.11 (0.00 - 4.44), n = 13	1.11 (0.00 - 2.22), n = 11	0.807
-pupillomotor	N/A	2.00 (0.33 - 3.00), n = 13	1.00 (0.00 - 3.67), n = 11	0.145

IgG	N/A	11.67 (8.77 - 16.18), n = 11	10.43 (6.08 - 13.56), n = 11	0.061
IgG1	N/A	6.56 (4.73 - 8.21), n = 11	5.56 (3.73 - 6.67), n = 8	0.020
IgG2	N/A	4.76 (2.75 - 5.67), n = 11	3.53 (1.80 - 5.86), n = 8	0.272
IgG3	N/A	0.49 (0.19 - 1.13), n = 11	0.38 (0.18 - 0.54), n = 8	0.351
IgG4	N/A	0.32 (0.20 - 1.25), n = 11	0.22 (0.14 - 0.84), n = 8	0.057

124

125 **Culturing and Preparation of Cells**

126 Human monocytic U937 cells (ACC-5, DSMZ-German Collection of Microorganisms and Cell
127 Cultures GmbH) were cultured in VLE RPMI 1640 medium (Bio & Sell, #F1415) supplemented
128 with 10% heat-inactivated fetal calf serum (Bio & Sell #FCS-ULE1415), 100 U/ml penicillin,
129 and 100 µg/ml streptomycin (BioWest #L0022). The cells were incubated under sterile
130 conditions at 37 °C with 5% carbon dioxide in culture flasks. For stimulation experiments, U937
131 cells were seeded at a density of 2×10^6 cells/ml one hour before stimulation in 24-well plates
132 (Sarstedt, #83.3922500).

133

134 **Isolation of Human IgG**

135 Human IgG was isolated from the patient serum using affinity chromatography at room
136 temperature. Serum samples were diluted fourfold in binding buffer (20 mM Na₂HPO₄+20 mM
137 NaH₂PO₄, pH 7) and centrifuged at 10,000 x g for 10 minutes at 4 °C. The supernatant was
138 aspirated from below the lipid layer and transferred to a fresh tube. HiTrap protein G Sepharose
139 columns (Cytiva, Sweden, #17040401) were equilibrated with binding buffer, and the diluted
140 serum was passed through the columns. Unbound molecules were washed out, and bound
141 IgG was eluted using 100 mM glycine (pH 2.7). The eluate was immediately neutralized with
142 1 M TRIS buffer, then diluted with PBS (BioWest, #L0615) to 15 ml and passed through
143 centrifugal filter units (Amicon, #UFC901024) at 3,000 g and 4 °C. After replenishing and re-
144 centrifuging, the retentate, the IgG concentration was measured using Bradford's reagent
145 (BioRad #5000006) according to the manufacturer's instructions.

146

147 **Stimulation of U937 Cells with IgG from Patients and Healthy Controls**

148 For stimulation experiments, U937 cells were exposed to purified IgG from three groups:
149 a) nPCS, b) pcME/CFS, and c) COVID-recovered HC. 6.67 µM IgG preparation was added to
150 the cells [13]. After stimulation for 24h, the cells were centrifuged, and the supernatants were
151 stored at -20 °C for cytokine analysis. The levels of cytokines in the supernatants were
152 analyzed using cytokine antibody array glass chips
153 (RayBiotech, Norcross, GA, USA, #AAH-CYT-G5-8). The array protocol was followed as per

154 the manufacturer's instructions: Non-specific binding sites on the chamber slides were blocked
155 using a blocking buffer. Following this, the supernatants were incubated on the slides with a
156 biotinylated antibody cocktail. After multiple washes, streptavidin-fluorochrome reagent HiLyte
157 Plus™ Fluor 555 was added. The slides were then laser-scanned at 532 nm using an Innoscan
158 Microarray Scanner (Innopsys, France). Background signals were subtracted, and the signals
159 were normalized to positive controls before further analysis using Agilent Scan Control
160 Software ver9.1.

161

162 **Data Preparation**

163 Data preparation was performed using the array manufacturer's batch correction tool available
164 at RayBiotech's online platform. Raw signals were first corrected for background by subtracting
165 the median background intensities. Subsequently, signal normalization was performed. To
166 normalize distribution and stabilize variance, the data underwent log₂ transformation. Further
167 processing of the data was performed using the limma package in R software to eliminate non-
168 biological variance between different experimental batches. This additional step enhanced the
169 reliability of subsequent statistical analyses, enabling the detection of meaningful biological
170 signals amidst technical variability.

171

172 **Statistical Analysis**

173 Descriptive Statistics were conducted to characterize the study groups, using medians and
174 ranges for numerical data due to the small sample size. For exploratory univariate analyses,
175 non-parametric tests were applied, including Kruskal-Wallis tests and Mann-Whitney *U* tests.
176 Principal Component Analysis (PCA) was performed on the batch-corrected dataset to explore
177 variance structure and clustering among the PCS, pcME/CFS, nPCS, and HC groups. PCA
178 plots provided a visual representation of the separation between groups, highlighting clustering
179 patterns. PCA visualizations were generated using the ggplot2 package in R. Linear Modeling
180 was conducted to identify cytokines with differential expression between groups using the
181 limma package. Comparisons included PCS versus HC, pcME/CFS versus nPCS, pcME/CFS
182 versus HC, and nPCS versus HC. Volcano plots were generated to visualize these differential
183 expression patterns, highlighting cytokines with statistically significant fold changes, defined
184 as an absolute log-fold change greater than one, with a significance level set at 10%, due to
185 the exploratory nature of the study.

186 **Correlation analysis** was performed to examine pairwise relationships between cytokines, as
187 well as between cytokines and clinical scores, as well as anti SARS-CoV2-Nukleocapsid
188 (NCAP) IgG and anti SRAS-CoV2-Spike Protein IgG utilizing Spearman's rank correlation
189 coefficient. This non-parametric approach was chosen to capture both linear and non-linear
190 associations, providing insights into co-regulatory mechanisms within the immune network.

191 Correlation matrices were generated separately for pcME/CFS, nPCS, and HC groups,
192 allowing for the identification of unique interaction patterns within each study group. Heatmaps,
193 created by using the ggplot2 package, provided a detailed visual summary of immune
194 interactions in the three groups. Significant correlations are marked with [*] for $p \leq 0.01$. The
195 classification of the correlation coefficient effect size is set as follows, values between 0 and
196 0.2 indicate no or a very small effect, from 0.2 up to 0.5 correspond to a small effect, while
197 values from 0.5 up to 0.8 signify a medium effect. Any value from 0.8 and above represents a
198 strong effect. All statistical analyses and visualizations were conducted in R (version 4.2.1) by
199 using RStudio (version 7.1), leveraging specialized packages tailored for each analysis step.

200

201 **Rational defining surrogate cytokine marker**

202 Cytokines appearing in the volcano plots with an absolute log-fold change greater than one
203 and a corresponding p-value below 10%, or those identified through a Kruskal-Wallis test with
204 a p-value below 10%, were selected as relevant candidates for further analysis.

205

206 **KEGG Analysis**

207 Kyoto Encyclopedia of Genes and Genomes (KEGG) was implemented to understand disease
208 pathogenesis through its detailed pathway maps and databases. For our study, surrogate
209 cytokines with significant correlations, as shown in **Figure 3**, were used as input for KEGG
210 pathway analysis (<https://www.genome.jp/kegg>) to identify biologically and clinically relevant
211 pathways.

212

213

214 **Results**

215 **The IgG-induced secretome discovered differences in PCS groups and in response to** 216 **viral proteins**

217 After stimulation with purified IgG, the cytokine profiles of monocytic U937 cells were analyzed
218 by a cytokine array comprising 80 different proteins. To measure AAB-induced cytokine
219 expression between HC and diseased cohorts, principal component analysis (PCA) was
220 employed to stratify high-dimensional data and to uncover distinct cytokine profiles, which
221 could contribute to group separations. Study groups were matched for a similar age distribution
222 and disease duration (**Table 1**). The BMI was not different among the groups. Our data indicate
223 a distinct clustering pattern across the groups (**Figure 1**). When comparing HC to all PCS
224 patients, including those with and without ME/CFS, a clear separation between the two cohorts
225 was identified (**Figure 1A**). Comparison of nPCS versus pcME/CFS demonstrated partially
226 overlapping clustering (**Figure 1B**), indicating shared immune dysregulation while also
227 capturing subgroup-specific immune patterns. PCS is characterized by an abnormal immune
228 response to SARS-CoV-2. To understand the differences in IgG-induced cytokine profiles
229 concerning specific antibodies against SARS-CoV-2 proteins, IgG-induced cytokines were
230 clustered according to the antibodies directed to SARS-CoV-2-spike and SARS CoV2- SARS-
231 CoV2-NCAP. Here, only significantly upregulated cytokines were selected. Interestingly,
232 SARS-CoV-2-specific antibodies did reveal the strongest correlations with IgG-induced
233 cytokines by applying HC-IgG. As examples, spike IgG antibody levels did positively correlate
234 with GRO- α (Growth-Regulated Oncogene Alpha; 0.72, $p = 0.01$), IL-7
235 (Interleukin 7; 0.68, $p = 0.01$), and IL-5 (Interleukin 5; 0.67, $p = 0.02$). Additionally, positive
236 correlations with antibody levels against SARS-CoV2-NCAP were shown with IGFBP-4
237 (Insulin-Like Growth Factor Binding Protein 4; 0.74, $p = 0.26$), IL-4
238 (Interleukin 4; 0.74, $p = 0.26$), and SCF (Stem Cell Factor; 0.74, $p = 0.26$), suggesting well-
239 regulated immune communication (**Figure 1C**). In contrast, cytokine correlations with SARS-
240 CoV-2 spike IgG were markedly absent in nPCS with only a positive correlation with NT-4
241 (0.59; $p =$) and a negative correlation with TGF- β 3 (Transforming Growth Factor Beta 3) levels
242 (-0.61, $p = 0.04$). In the pcME/CFS group (**Figure 1C**), strong negative correlations between
243 spike IgG titers and NAP-2 (-0.90, $p = 0.00$), MCP-3 (-0.81, $p = 0.03$), and MIP-3 α
244 (-0.75, $p = 0.03$) levels were detected as well as between SARS-CoV2-NCAP IgG ab levels
245 and MCP-3 levels (-0.81, $p = 0.03$). These data indicate changes in regulatory mechanisms
246 induced by SARS-CoV-2 and a disturbed immune response compared to HC
247 (**Figure 1C, nPCS**).

248

249

250

251 **nPCS and pcME/CFS AABs mediate distinct cytokine profiles compared to HC.**

252 Volcano plots illustrate significant differences in the IgG-induced cytokine expression between
253 patients and HC. Comparing PCS with HC (**Figure 2A**), several cytokines had exhibited
254 significant upregulation such as MIP-1d (Macrophage Inflammatory Protein-1d), PDGF-BB
255 (Platelet-Derived Growth Factor-BB), TGF- β 3, and SCF (Stem Cell Factor), all of which had
256 shown both a high log₂ fold change and statistically significant p-values. These cytokines are
257 involved in inflammatory, fibrotic, and tissue repair pathways, suggesting persistent immune
258 activation. Further, in PCS, PIGF (Placental Growth Factor), MCP-2 (Monocyte Chemotactic
259 Protein-2), and IL-4 have been also upregulated as markers for angiogenesis, monocyte
260 recruitment, and Th2-related anti-inflammatory responses. Thrombopoietin, a marker for
261 disruptions in coagulation, was modestly upregulated. The IgG-induced secretome also
262 showed differences between pcME/CFS and nPCS (**Figure 2B**). Specifically, IL-1 α
263 (Interleukin-1 alpha), GRO- α (Growth-Regulated Oncogene alpha), and Eotaxin-3
264 (Eosinophil Chemotactic Protein 3) revealed notable increases in expression in pcME/CFS.
265 The detailed comparison between nPCS or pcME/CFS with HC exhibited minor differences in
266 the expression patterns (**Figure 2C and D**). MIP-1 δ , IL-4 and TGF- β 3, revealed comparable
267 upregulation in nPCS as well in pcME/CFS groups compared to HC, suggesting shared
268 features in PCS regardless of ME/CFS status. Interestingly, in the nPCS group compared to
269 HC, a downregulated cytokine levels of GRO- α , IL-5 and IL-7 were found (**Figure 2C**).

270

271 **AAB-induced secretome identified distinct correlations between cytokines and**
272 **pathways among the different groups.**

273 Intra-cytokine correlations showed marked differences as illustrated in **Figure 3**. In HC, only a
274 few strong correlations such as between FGF-9 and MDC levels ($r = 0.90$; $p < 0.001$), between
275 Gro-a and IL-5 as well as IFN-g and TGF-b1 (both $r = 0.84$; $p < 0.001$), (**Figure 3A**). Pathway
276 analysis for HC of the AAB-induced monocyte secretome (**Figure 3B**) revealed a minor
277 number of cytokines involved in autoimmune or infectious disease-related pathways,
278 underscoring the homeostatic nature of HC cytokine interactions. In nPCS (**Figure 3C**),
279 AAB-induced monocyte secretomes reflected altered immune signaling, with strong positive
280 correlations between cytokine levels of IL-15 and IL-5 ($r = 0.99$ $p < 0.001$), GDNF and IGF-I
281 ($r = 0.94$; $p < 0.001$), IL-15 and IL-7 ($r = 0.94$; $p < 0.001$) and NAP-2 and PDGF-BB
282 ($r = 0.90$; $p < 0.001$). Pathways associated with viral infections and rheumatoid arthritis were
283 found, alongside IL-17 signaling pathways. These pathways suggest an overlap between
284 pcME/CFS immune dysregulation and inflammatory responses commonly observed in viral
285 and autoimmune conditions (**Figure 3D**). In pcME/CFS (**Figure 3E**), unique cytokine
286 correlations were found between IL-15 and TNF-b ($r = 0.99$; $p < 0.001$), IFN-g and TGF-b1
287 ($r = 0.97$; $p < 0.001$), FGF-9 and PIGF ($r = 0.95$; $p < 0.001$) and FGF-9 and

288 MIP-3a ($r = 0.91$; $p < 0.001$). Pathway analysis of these cytokine networks (**Figure 3F**) revealed
289 strong functional enrichments in pathways associated with rheumatoid arthritis and
290 inflammatory bowel disease, cytokine signaling in viral infection. These findings suggest that
291 pcME/CFS-associated AABs drive immune networks with significant overlap to chronic
292 inflammatory and viral infection-related pathways. In both diseased groups, strong correlations
293 were found between IL-5 and IL-7 (nPCS, 0.95 ; $p < 0.001$ / pcME/CFS, $r = 0.99$; $p < 0.001$).
294 Also, moderate correlations in both groups were observed between BDNF (Brain-Derived
295 Neurotrophic Factor) and LIGHT, (nPCS, $r = 0.86$; $p < 0.001$; pcME/CFS $r = 0.88$; $p < 0.001$).
296 Noteworthy, in both PCS groups (**Figure 3D, F**) significant fold enrichments were found for
297 RAS-signaling pathways. Cytokine-receptor interactions were found in all groups resembling
298 the nature of cytokine data submitted to KEGG analysis. In sum, the data underscore the
299 critical role of IgG-induced monocyte secretomes in driving disease-specific cytokine
300 interactions and signaling networks.

301

302 **IgG-induced proteins correlate with distinct manifestations in nPCS and pcME/CFS.**

303 To explore how IgG-driven cytokine responses may contribute to specific symptoms,
304 IgG-induced protein levels were compared with clinical data (**Figure 4**). In nPCS (**Figure 4 A**),
305 moderate positive correlations were found between cytokine levels and symptom severity
306 (Bell score). Autonomic dysfunction assessed by the total Composite Symptom Score
307 (Compass-31 total), correlated significantly with Eotaxin levels ($r = 0.60$, $p = 0.03$), indicating
308 its role in exacerbating symptoms and eosinophil recruitment [26]. In more detail, the domain
309 bladder impairment (Compass-31) showed strong correlations with IGFBP-4 levels
310 ($r = 0.75$, $p < 0.001$), PIGF ($r = 0.69$, $p = 0.01$), and MCP-2 levels ($r = 0.63$, $p = 0.02$), reflecting
311 the involvement of neuroprotective mechanisms, vascular inflammation, and monocyte
312 recruitment in nPCS bladder symptoms [27-29]. Remarkably, severity of fatigue were positively
313 correlated with IL-4 levels ($r = 0.66$, $p = 0.01$), emphasizing Th2-mediated immune activation
314 [30] as well as with FGF-9 levels ($r = 0.72$, $p = 0.01$). Eotaxin levels were moderately correlated
315 with the degree autonomic dysfunction ($r = 0.6$, $p = 0.03$). In nPCS, gastrointestinal symptoms
316 (com_gi) were negatively associated with RANTES levels ($r = -0.79$, $p < 0.001$) and NAP-2
317 levels ($r = -0.68$, $p = 0.01$), indicating the role of impaired monocyte chemotactic signaling in
318 eosinophil regulation [31].

319 In pcME/CFS (**Figure 4B**), unique cytokine correlations suggested heightened
320 neuroinflammatory and immune dysregulation compared to nPCS. The levels of RANTES,
321 involved in angiogenesis as well as in inflammation, were strongly correlated positively with
322 both the Bell Disability Score ($r = 0.72$, $p = 0.01$) and bladder dysfunction (com_blad)
323 ($r = 0.71$, $p = 0.01$) [32]. Correlations between the Immune Score and the levels of the
324 neurotrophin NT4 ($r = 0.68$, $p = 0.02$) were observed. Interestingly, severity of fatigue was

325 correlated with Thrombopoietin levels ($r = 0.62$, $p = 0.04$), implicating platelet activation in
326 fatigue and chronic inflammation [33]. Additionally, levels of IGFBP-4 ($r = 0.61$, $p = 0.05$), a
327 neuronal survival factor [27], was correlated positively with the severity of muscle pain. The
328 degree of cognitive dysfunctions was correlated negatively with GRO- α ($r = -0.67$, $p = 0.02$),
329 while IL-7 levels negatively correlated with muscle pain severity ($r = -0.60$, $p = 0.05$). The levels
330 of the chemokine MCP-2, found increased in PCS patients [29] and causing endothelial
331 impairment [34], was correlated particularly with orthostatic dysfunction ($r = 0.68$; $p = 0.02$) and
332 compass-31 (com_total; $r = 0.62$, $p = 0.05$). In pcME/CFS, neuroinflammatory markers had
333 shown stronger negative correlations compared to nPCS. IL-1 α correlated negatively with
334 severity of headache ($r = -0.82$, $p < 0.001$), suggesting its role in neuroinflammation linked to
335 headache symptoms. TGF- β 1 also had shown negative correlations with headache severity
336 ($r = -0.62$, $p = 0.04$), alterations of regulatory signaling in pcME/CFS [31].

337

338 **Discussion**

339 In this study, we aimed to identify common and distinct IgG-driven immune mechanisms, by
340 stimulating monocytes, a supposed key cell in the response to virus infections, with IgG from
341 nPCS and pcME/CFS patients [13, 16, 35]. The observed differences in the responses to viral
342 proteins indicate disturbed immune response already present at the beginning of PCS. In
343 general, PCS patients exhibit distinct patterns of cytokine upregulation associated with immune
344 dysregulation, tissue repair, and chronic inflammation. In addition, key differences between
345 nPCS and pcME/CFS were identified, suggesting that IgG from pcME/CFS patients exhibit
346 more pronounced neurotrophic responses. IgG-induced cytokines exhibit strong correlations
347 with clinical symptoms emphasizing similarities between IgG-induced pathways and those
348 present in the patients. The results of this study strongly indicate a contribution of AAB in the
349 pathogenesis of disease and provide important insights into the immune landscape of PCS.
350 The study highlights potential pathways involved in the persistence of symptoms and the
351 development of chronic fatigue-related conditions.

352

353 In pcME/CFS, AABs mediated strong inflammatory and neurotrophic cytokines indicating
354 immune and endothelial dysregulation. The significant upregulation of cytokines such as
355 MIP-1d, PDGF-BB, and TGF- β 3 in PCS patients points to persistent immune dysregulation by
356 AABs months after the acute phase of SARS-CoV-2 infection. These proteins are implicated
357 in tissue repair and fibrosis, aligning with recent findings that suggest long-term tissue damage
358 and scarring may be prominent features of PCS [36]. The upregulation of PIGF further supports
359 the hypothesis of ongoing vascular and immune disturbances in PCS patients caused by
360 dysregulation of the autoantibodiome. PIGF has been associated with vascular inflammation
361 and angiogenesis, both of which may contribute to chronic symptoms such as fatigue and

362 shortness of breath observed in PCS patients [8]. The increased levels of IL-4 indicate a mixed
363 immune response, where both pro-inflammatory and regulatory pathways are activated, may
364 reflecting the complex nature of immune recovery in PCS. Moreover, the moderate
365 upregulation of Thrombopoietin may suggest the involvement of platelet activation and
366 coagulation pathways or a negative rebound causing thrombocytopenia, which have been
367 implicated in both acute COVID-19 and long-COVID syndromes [33]. This could contribute to
368 microvascular dysfunction, further exacerbating symptoms such as brain fog and fatigue.
369 By distinguishing the immune response to IgG between nPCS to pcME/CFS the upregulation
370 of IL-1 α , GRO- α , and Eotaxin-3 in pcME/CFS patients aligns with previous studies that have
371 demonstrated immune dysregulation and heightened inflammation in ME/CFS compared to
372 nPCS groups. These cytokines are critical mediators of inflammation, which could contribute
373 to the severe fatigue, post-exertional malaise, and other hallmark symptoms of ME/CFS [37].
374 pcME/CFS-IgG triggered cytokine profile also reflects a shift toward a more chronic
375 inflammatory state, GRO- α is linked to neutrophil activation and could be contributing to
376 chronic low-grade inflammation, while Eotaxin-3 suggests a potential role for eosinophils,
377 which are involved in allergic responses but also implicated in prolonged inflammatory states
378 [26, 38]. The relatively stable levels of TGF- β 1 in this cohort could point to a lack of sufficient
379 regulatory immune responses, which was partly observed in in-vitro experiments with PCS
380 ME/CFS sera, where immune dysfunction persists, additionally resembled by sICAM-1,
381 IGFBPB-4 and cystatin-C [8]. These findings provide crucial insights into the very early
382 AAB-mediated processes occurring in PCS, particularly for patients with ME/CFS. The short-
383 term nature of the experiments enables us to observe immune dysregulation at the onset of
384 the post-viral phase rather than long-term chronic responses.

385 The results of group specific cytokine correlations highlight distinct cytokine and growth factor
386 interactions in nPCS and pcME/CFS, shedding light on immune mechanisms underlying
387 symptom severity and disease progression. In both groups, while strongest correlations were
388 observed in pcME/CFS, for cytokines such as IL-5, IL-7, IL-15, and TNF- β , reflecting enhanced
389 inflammatory and immune dysregulation. IL-15, associated with disease severity in COVID-19
390 [39] and TNF- β , a key marker uniquely elevated in ME/CFS after exercise[40], point to chronic
391 immune dysregulation and post-exertional inflammation, characteristic of pcME/CFS. These
392 findings suggest a sustained and amplified immune response compared to pcME/CFS. Growth
393 factors such as FGF-9 and PIGF also exhibited stronger associations in pcME/CFS. FGF-9,
394 documented in movement disorders and ME/CFS, plays a role in tissue repair and is implicated
395 in pulmonary fibrosis [41], while PIGF is linked to angiogenesis and increased after acute
396 exercise [42]. Together with pathway correlations with autoimmune diseases and
397 RAS-signaling, the results indicate angiogenic and fibrotic dysregulations, contributing to
398 tissue remodeling and symptom chronicity in pcME/CFS. These results underscore the

399 importance of cytokines and growth factors induced by patient IgG in both the severity and
400 progression of PCS.

401

402 The comparative analysis of the AAB-induced secretome revealed distinct immune pathways
403 underlying symptom manifestations in nPCS and pcME/CFS. These findings emphasize the
404 central role of immune dysregulation in driving fatigue, cognitive dysfunction, and organ-
405 specific symptoms, highlighting the differing contributions of pro-inflammatory and
406 neuroprotective cytokines in these conditions. In nPCS, immune dysregulation was linked to
407 symptom severity, with cytokines such as Eotaxin and IGFBP-4 prominently associated with
408 overall symptom burden and bladder dysfunction, respectively. Eotaxin, involved in eosinophil
409 recruitment and monocyte-driven inflammation, correlated positively with symptom severity,
410 reflecting its role in immune-mediated exacerbation [31]. IGFBP-4, recognized for its
411 neuroprotective properties, showed a strong positive correlation with bladder dysfunction,
412 suggesting a compensatory response to immune-mediated damage in bladder tissues [27].
413 Thrombopoietin was negatively associated with post-exertional malaise (PEM), linking platelet
414 activation to vascular repair and immune recovery processes [33]. Similarly, RANTES and
415 NAP-2 exhibited negative correlations with gastrointestinal symptoms, reflecting impaired
416 chemotactic signaling and vascular regulation [31, 43]. The pcME/CFS demonstrated
417 heightened immune dysregulation and stronger associations with neuroinflammatory and
418 neuroprotective pathways. RANTES emerged as a dual mediator, positively correlating with
419 bladder dysfunction but better physical function (high Bell score), suggesting its involvement
420 in tissue repair and neuroimmune pathways specific to severe ME/CFS [32]. In fibromyalgia
421 syndrome, where muscle pain and bladder issues coexist, the association of IGFBP-4 with
422 muscle pain points to shared inflammatory pathways [44]. These findings highlight a
423 neuroimmune axis driven by monocytes in response to AABs in both pain and autonomic
424 dysfunction. Noteworthy, bladder function did not correlate with the age of pcME/CFS patients.
425 Neurotrophic factors such as NT4 and PDGF-BB were positively correlated with immune
426 scores, which may indicate compensatory responses to ongoing neuroinflammation and tissue
427 damage, both effectors promote survival of different immune cells [31, 45]. Fatigue in
428 pcME/CFS showed nuanced cytokine interactions. While IL-4 and MCP-2 were positively
429 associated with fatigue, TGF- β 1 exhibited a negative correlation, reflecting its protective role
430 in regulating immune-driven fatigue [31, 46]. Intriguingly, MCP-2 upregulation is well described
431 in PCS patients, hypothesizing a key role of AAB-mediated monocytic response in PCS
432 pathogenesis [29]. Neuroinflammation was evident through negative correlations between
433 cognitive function and cytokines such as Eotaxin and GRO- α , emphasizing the impact of
434 chronic inflammation on cognitive impairment [26, 27].

435 This study demonstrated IgG-induced cytokine signatures in an in vitro assay correlate more
436 pronounced with disease-specific symptoms compared to direct serum AAB measurements or
437 analyses of specific antibodies, such as β 2-adrenergic receptor antibodies in ME/CFS [14, 16].
438 These findings suggest that IgG-induced cytokine responses provide a more accurate
439 assessment of pathogenic potential. An in vitro diagnostic developed in parallel by the Clinic
440 for Rheumatology and Clinical Immunology (University Clinic Schleswig-Holstein; placeholder
441 (EP25150270.4) further validated these results, showing a sensitivity of 92% and specificity of
442 83% in distinguishing PCS patients from HC, and for the first time differentiating nPCS from
443 PCME/CFS patients. This approach highlights its potential for precise diagnosis and disease
444 prognosis.

445 **Conclusion**

446 The findings from this study suggest that the immune exhaustion observed in monocytes
447 stimulated by IgG from nPCS and pcME/CFS patients could be driven by chronic activation
448 through dysregulated AABs. This has been observed in other chronic inflammatory conditions,
449 where persistent immune stimulation, like viral infections, lead to immune cell exhaustion and
450 endothelial impairment [47-49]. Thus, AABs may maintain a state of chronic immune activation,
451 which, over time, results in monocyte dysfunction and dedifferentiation, mirroring processes
452 seen in autoimmune diseases and chronic infections [50, 51], subsequently contributing to
453 immune exhaustion and causing long-term symptoms observed in PCS with ME/CFS.

454

455

456 References

- 457 1. Davis, H.E., et al., *Characterizing long COVID in an international cohort: 7 months of symptoms*
458 *and their impact*. eClinicalMedicine, 2021. **38**: p. 101019.
- 459 2. Xie, Y., B. Bowe, and Z. Al-Aly, *Burdens of post-acute sequelae of COVID-19 by severity of acute*
460 *infection, demographics and health status*. Nat Commun, 2021. **12**(1): p. 6571.
- 461 3. Logue, J.K., et al., *Sequelae in Adults at 6 Months After COVID-19 Infection*. JAMA Netw Open,
462 2021. **4**(2): p. e210830.
- 463 4. Kedor, C., et al., *A prospective observational study of post-COVID-19 chronic fatigue syndrome*
464 *following the first pandemic wave in Germany and biomarkers associated with symptom*
465 *severity*. Nat Commun, 2022. **13**(1): p. 5104.
- 466 5. Nacul, L., et al., *European Network on Myalgic Encephalomyelitis/Chronic Fatigue Syndrome*
467 *(EUROMENE): Expert Consensus on the Diagnosis, Service Provision, and Care of People with*
468 *ME/CFS in Europe*. Medicina (Kaunas), 2021. **57**(5).
- 469 6. Bonilla, H., et al., *Myalgic Encephalomyelitis/Chronic Fatigue Syndrome is common in post-*
470 *acute sequelae of SARS-CoV-2 infection (PASC): Results from a post-COVID-19 multidisciplinary*
471 *clinic*. Front Neurol, 2023. **14**: p. 1090747.
- 472 7. Mejia-Renteria, H., et al., *In-vivo evidence of systemic endothelial vascular dysfunction in*
473 *COVID-19*. Int J Cardiol, 2021. **345**: p. 153-155.
- 474 8. Flaskamp, L., et al., *Serum of Post-COVID-19 Syndrome Patients with or without ME/CFS*
475 *Differentially Affects Endothelial Cell Function In Vitro*. Cells, 2022. **11**(15).
- 476 9. Haffke, M., et al., *Endothelial dysfunction and altered endothelial biomarkers in patients with*
477 *post-COVID-19 syndrome and chronic fatigue syndrome (ME/CFS)*. J Transl Med, 2022. **20**(1):
478 p. 138.
- 479 10. Wang, E.Y., et al., *Diverse functional autoantibodies in patients with COVID-19*. Nature, 2021.
480 **595**(7866): p. 283-288.
- 481 11. Rodriguez-Perez, A.I., et al., *Autoantibodies against ACE2 and angiotensin type-1 receptors*
482 *increase severity of COVID-19*. J Autoimmun, 2021. **122**: p. 102683.
- 483 12. Cabral-Marques, O., et al., *GPCR-specific autoantibody signatures are associated with*
484 *physiological and pathological immune homeostasis*. Nat Commun, 2018. **9**(1): p. 5224.
- 485 13. Yue, X., et al., *Induced antibodies directed to the angiotensin receptor type 1 provoke skin and*
486 *lung inflammation, dermal fibrosis and act species overarching*. Ann Rheum Dis, 2022. **81**(9):
487 p. 1281-1289.
- 488 14. Freitag, H., et al., *Autoantibodies to Vasoregulative G-Protein-Coupled Receptors Correlate*
489 *with Symptom Severity, Autonomic Dysfunction and Disability in Myalgic*
490 *Encephalomyelitis/Chronic Fatigue Syndrome*. J Clin Med, 2021. **10**(16).
- 491 15. Bynke, A., et al., *Autoantibodies to beta-adrenergic and muscarinic cholinergic receptors in*
492 *Myalgic Encephalomyelitis (ME) patients - A validation study in plasma and cerebrospinal fluid*
493 *from two Swedish cohorts*. Brain Behav Immun Health, 2020. **7**: p. 100107.
- 494 16. Sotzny, F., et al., *Dysregulated autoantibodies targeting vaso- and immunoregulatory*
495 *receptors in Post COVID Syndrome correlate with symptom severity*. Front Immunol, 2022. **13**:
496 p. 981532.
- 497 17. Merad, M. and J.C. Martin, *Author Correction: Pathological inflammation in patients with*
498 *COVID-19: a key role for monocytes and macrophages*. Nat Rev Immunol, 2020. **20**(7): p. 448.
- 499 18. Ye, Q., B. Wang, and J. Mao, *The pathogenesis and treatment of the 'Cytokine Storm' in COVID-*
500 *19*. J Infect, 2020. **80**(6): p. 607-613.
- 501 19. Hu, W.T., et al., *Clinical and CSF single-cell profiling of post-COVID-19 cognitive impairment*.
502 Cell Rep Med, 2024. **5**(5): p. 101561.
- 503 20. Bell, D.S., *The Doctor's Guide To Chronic Fatigue Syndrome: Understanding, Treating, And Living*
504 *With Cfids*. 1994: Da Capo Press.
- 505 21. Cotler, J., et al., *A Brief Questionnaire to Assess Post-Exertional Malaise*. Diagnostics (Basel),
506 2018. **8**(3).

- 507 22. Cella, M. and T. Chalder, *Measuring fatigue in clinical and community settings*. J Psychosom
508 Res, 2010. **69**(1): p. 17-22.
- 509 23. Sletten, D.M., et al., *COMPASS 31: a refined and abbreviated Composite Autonomic Symptom*
510 *Score*. Mayo Clin Proc, 2012. **87**(12): p. 1196-201.
- 511 24. Harris, P.A., et al., *Research electronic data capture (REDCap)--a metadata-driven*
512 *methodology and workflow process for providing translational research informatics support*. J
513 Biomed Inform, 2009. **42**(2): p. 377-81.
- 514 25. Harris, P.A., et al., *The REDCap consortium: Building an international community of software*
515 *platform partners*. J Biomed Inform, 2019. **95**: p. 103208.
- 516 26. Ravensberg, A.J., et al., *Eotaxin-2 and eotaxin-3 expression is associated with persistent*
517 *eosinophilic bronchial inflammation in patients with asthma after allergen challenge*. J Allergy
518 Clin Immunol, 2005. **115**(4): p. 779-85.
- 519 27. Son, J.W., et al., *Glia-Like Cells from Late-Passage Human MSCs Protect Against Ischemic Stroke*
520 *Through IGFBP-4*. Mol Neurobiol, 2019. **56**(11): p. 7617-7630.
- 521 28. Scott, X.O., et al., *Cohort study on the differential expression of inflammatory and angiogenic*
522 *factors in thrombi, cerebral and peripheral plasma following acute large vessel occlusion*
523 *stroke*. J Cereb Blood Flow Metab, 2022. **42**(10): p. 1827-1839.
- 524 29. Mahdi, A., et al., *Dysregulations in hemostasis, metabolism, immune response, and*
525 *angiogenesis in post-acute COVID-19 syndrome with and without postural orthostatic*
526 *tachycardia syndrome: a multi-omic profiling study*. Scientific Reports, 2023. **13**(1): p. 20230.
- 527 30. Wang, J., et al., *Pathogenesis of allergic diseases and implications for therapeutic interventions*.
528 Signal Transduct Target Ther, 2023. **8**(1): p. 138.
- 529 31. Vargas-Leal, V., et al., *Expression and function of glial cell line-derived neurotrophic factor*
530 *family ligands and their receptors on human immune cells*. J Immunol, 2005. **175**(4): p. 2301-
531 8.
- 532 32. Miłcarska, S., et al., *Assessment of the RANTES Level Correlation and Selected Inflammatory*
533 *and Pro-Angiogenic Molecules Evaluation of Their Influence on CRC Clinical Features: A*
534 *Preliminary Observational Study*. Medicina (Kaunas), 2022. **58**(2).
- 535 33. Ryan, F.J., et al., *Long-term perturbation of the peripheral immune system months after SARS-*
536 *CoV-2 infection*. BMC Med, 2022. **20**(1): p. 26.
- 537 34. Xue, S., et al., *C-C motif ligand 8 promotes atherosclerosis via NADPH oxidase 2/reactive*
538 *oxygen species-induced endothelial permeability increase*. Free Radical Biology and Medicine,
539 2021. **167**: p. 181-192.
- 540 35. Kawakami, A., N. Iwamoto, and K. Fujio, *Editorial: The role of monocytes/macrophages in*
541 *autoimmunity and autoinflammation*. Front Immunol, 2022. **13**: p. 1093430.
- 542 36. Melo, A.K.G., et al., *Biomarkers of cytokine storm as red flags for severe and fatal COVID-19*
543 *cases: A living systematic review and meta-analysis*. PLoS One, 2021. **16**(6): p. e0253894.
- 544 37. Giloteaux, L., et al., *Proteomics and cytokine analyses distinguish myalgic*
545 *encephalomyelitis/chronic fatigue syndrome cases from controls*. Journal of Translational
546 Medicine, 2023. **21**(1): p. 322.
- 547 38. Corbitt, M., et al., *A systematic review of cytokines in chronic fatigue syndrome/myalgic*
548 *encephalomyelitis/systemic exertion intolerance disease (CFS/ME/SEID)*. BMC Neurology,
549 2019. **19**(1): p. 207.
- 550 39. Bekbossynova, M., et al., *Unraveling Acute and Post-COVID Cytokine Patterns to Anticipate*
551 *Future Challenges*. Journal of Clinical Medicine, 2023. **12**(16): p. 5224.
- 552 40. Moneghetti, K.J., et al., *Value of Circulating Cytokine Profiling During Submaximal Exercise*
553 *Testing in Myalgic Encephalomyelitis/Chronic Fatigue Syndrome*. Scientific Reports, 2018. **8**(1):
554 p. 2779.
- 555 41. Sfera, A., et al., *Microbial Translocation Disorders: Assigning an Etiology to Idiopathic Illnesses*.
556 Applied Microbiology, 2023. **3**(1): p. 212-240.
- 557 42. Landers-Ramos, R.Q., et al., *Circulating angiogenic and inflammatory cytokine responses to*
558 *acute aerobic exercise in trained and sedentary young men*. European Journal of Applied
559 Physiology, 2014. **114**(7): p. 1377-1384.

- 560 43. Gleissner, C.A., P. von Hundelshausen, and K. Ley, *Platelet chemokines in vascular disease*.
561 *Arterioscler Thromb Vasc Biol*, 2008. **28**(11): p. 1920-7.
- 562 44. Furuta, A., et al., *Time-dependent changes in bladder function and plantar sensitivity in a rat*
563 *model of fibromyalgia syndrome induced by hydrochloric acid injection into the gluteus*. *BJU*
564 *Int*, 2012. **109**(2): p. 306-10.
- 565 45. Bohmwald, K., et al. *Neurotrophin Signaling Impairment by Viral Infections in the Central*
566 *Nervous System*. *International Journal of Molecular Sciences*, 2022. **23**, DOI:
567 10.3390/ijms23105817.
- 568 46. Blundell, S., et al., *Chronic fatigue syndrome and circulating cytokines: A systematic review*.
569 *Brain Behav Immun*, 2015. **50**: p. 186-195.
- 570 47. Petri, R.M., et al., *Activated Tissue-Resident Mesenchymal Stromal Cells Regulate Natural Killer*
571 *Cell Immune and Tissue-Regenerative Function*. *Stem Cell Reports*, 2017. **9**(3): p. 985-998.
- 572 48. Angelosanto, J.M., et al., *Progressive loss of memory T cell potential and commitment to*
573 *exhaustion during chronic viral infection*. *J Virol*, 2012. **86**(15): p. 8161-70.
- 574 49. Gao, Z., et al., *T-cell exhaustion in immune-mediated inflammatory diseases: New implications*
575 *for immunotherapy*. *Front Immunol*, 2022. **13**: p. 977394.
- 576 50. Heming, M., et al., *Neurological Manifestations of COVID-19 Feature T Cell Exhaustion and*
577 *Dedifferentiated Monocytes in Cerebrospinal Fluid*. *Immunity*, 2021. **54**(1): p. 164-175.e6.
- 578 51. Fagiolo, E. and C.T. Terenzi, *Enhanced IL-10 Production In Vitro by Monocytes in Autoimmune*
579 *Haemolytic Anaemia*. *Immunological Investigations*, 1999. **28**(5-6): p. 347-352.
- 580

581

582 **Funding**

583 Founded by BMBF (German ministry for education and research) project "Elucidating the
584 immune pathomechanisms of post-infectious ME/CFS (IMMME), funding number 01EJ2204C.

585

586 **Acknowledgments**

587 We are grateful to the patients who participated in this study despite their individual disease
588 related impairment.

589

590 **Conflict of interest**

591 The authors GR and AH hold a submitted patent for cytokine signature detecting Post-COVID
592 Syndrome, signatures for Post-COVID Syndrome with or without ME/CFS, respectively. The
593 authors declare that HH and KS-F are managing directors of CellTrend. CellTrend holds
594 together with Charité a patent for the diagnostic use of AABs against ADRB2. CS has a
595 consulting agreement with CellTrend. The remaining authors declare that the research was
596 conducted in the absence of any commercial or financial relationships that could be construed
597 as a potential conflict of interest.

598 **Table and figure Legends**

599 **Table 1.** Clinical scorings and cohort characterization. Continuous variables were expressed
600 as median and range. Univariate comparisons of study groups were done using the Kruskal–
601 Wallis test (three groups) or the Mann-Whitney-U-Test (two groups). A two-tailed p-value of
602 <0.01 was considered statistically significant. [n. a. = not assessed].

603 **Figure 1.** Identification of IgG-induced monocytic secretome in PCS patients compared to HC.
604 PCA analysis indicated that the two cohorts are distinct based on monocytic secretome
605 between PCS patients and HC (A) and between nPCS and pcME/CFS (B). The heatmap
606 revealed an association between spike or NCAP IgGs and secretome factors between nPCS,
607 pcME/CFS, and HC (C).

608 **Figure 2.** Exploration of cytokine expression between different groups: pcME/CFS&nPCS vs.
609 HC (A), pcME/CFS vs. PCS (B), nPCS vs. HC (C), and pcME/CFS vs. HC (D). The volcano
610 plot illustrates differences in cytokine expression between the groups after stimulation of
611 monocytic cells with IgG.

612 **Figure 3.** Correlations between cytokines and major signaling pathways in AAB-induced
613 monocyte secretome in HC (A), PCS (B), and pcME/CFS (C). The nodes in the graphs (A, C,
614 and E) represent variables (each cytokine), and a line between two nodes indicates
615 Spearman's rank correlation coefficient. The line width indicates the strength of the
616 association, with stronger correlations indicated by thicker lines. Multiple connections of nodes
617 indicate clustering between the variables. The bar plot (B, D, and F) indicates the 10 most
618 representative altered canonical KEGG pathways affected by the differentially expressed
619 cytokines. The most significantly enriched pathways are depicted in a progressively redder
620 colour.

621 **Figure 4.** The heat map of the correlation matrix summarizes the results of Spearman
622 correlation analysis among the clinical symptom scores and cytokine data considered in PCS
623 (A) and pcME/CFS (B). Spearman correlation coefficients (r) are indicated in the relative boxes
624 at the intersection between the considered variables. Positive and negative correlation
625 coefficients are shown in red and blue, respectively.

626

627

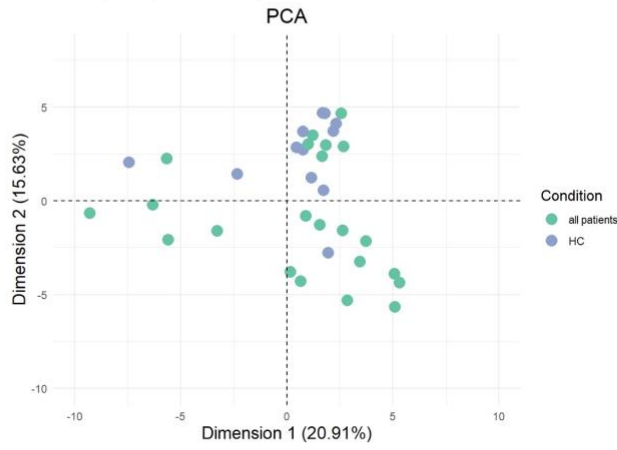
628

629

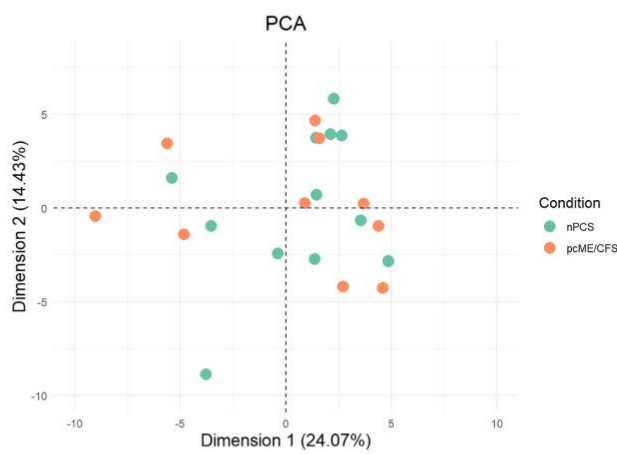
630

Figure 1

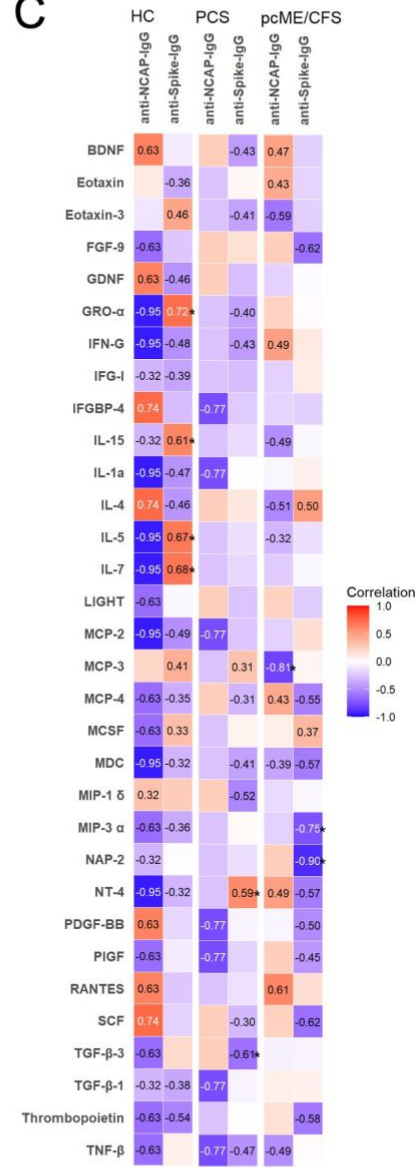
A PCS (all patients) vs. HC



B pcME/CFS vs. PCS



C



631

632

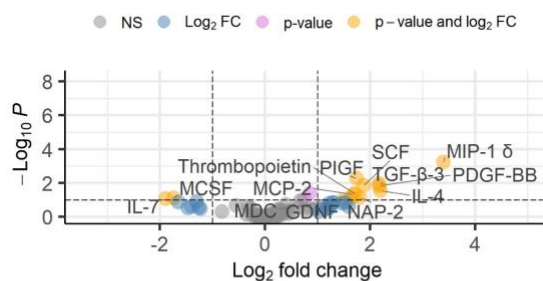
633

634

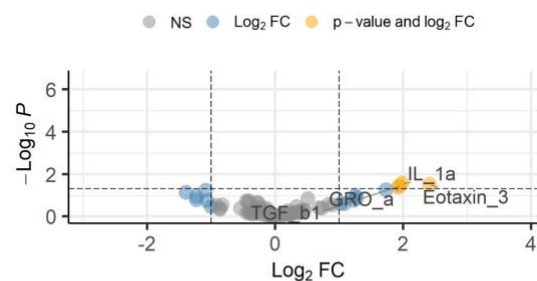
635

Figure 2

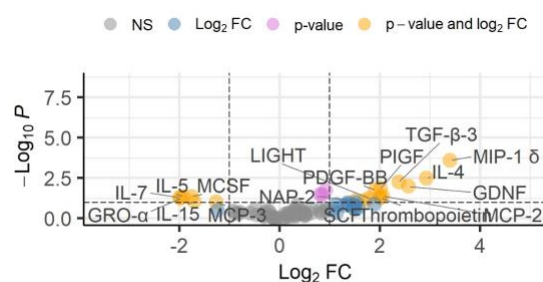
A PCS (all patients) vs. HC



B pcME/CFS vs. nPCS



C nPCS vs. HC



D pcME/CFS vs. HC



636

637

638

639

640

641

642

643

644

645

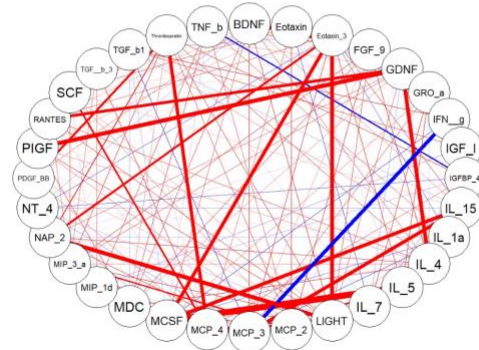
646

647

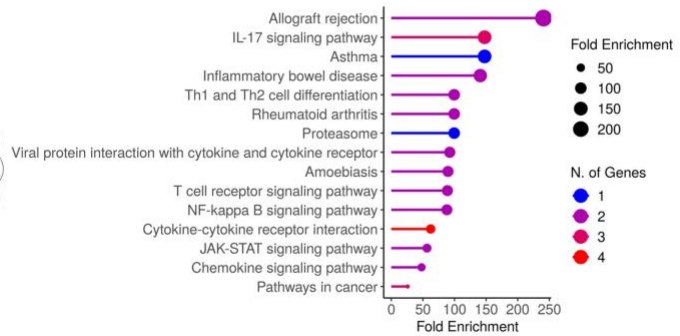
648

Figure 3

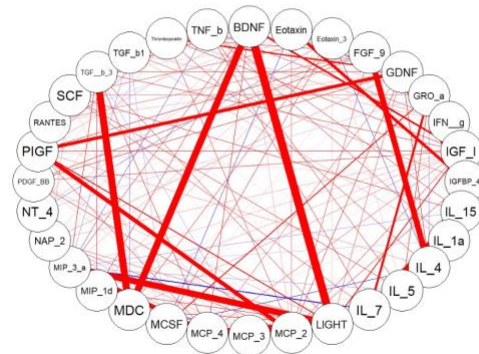
A HC Correlation of Cytokines



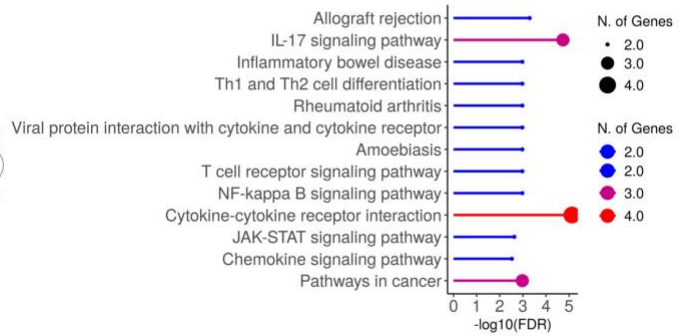
B HC KEGG



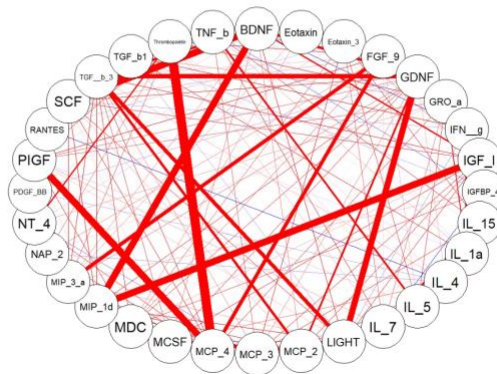
C nPCS Correlation of Cytokines



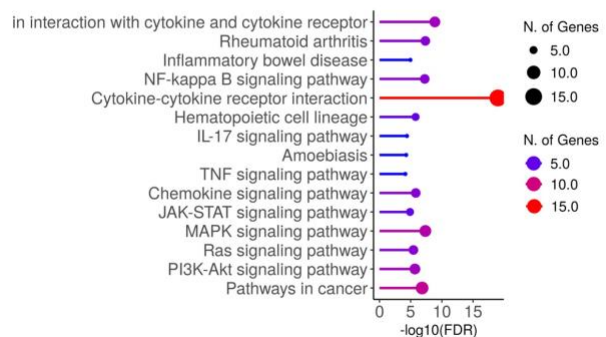
D nPCS KEGG



E pcME/CFS Correlation of Cytokines



F pcME/CFS KEGG



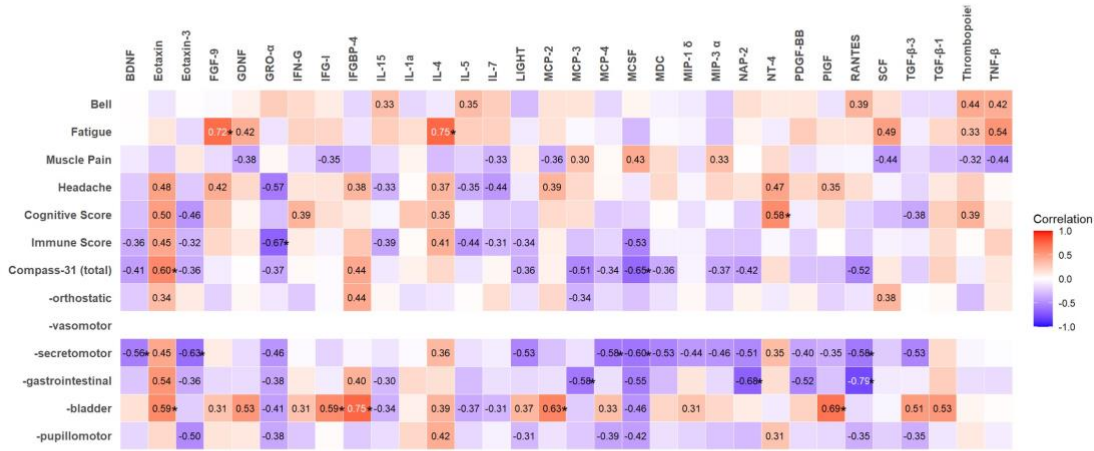
649

650

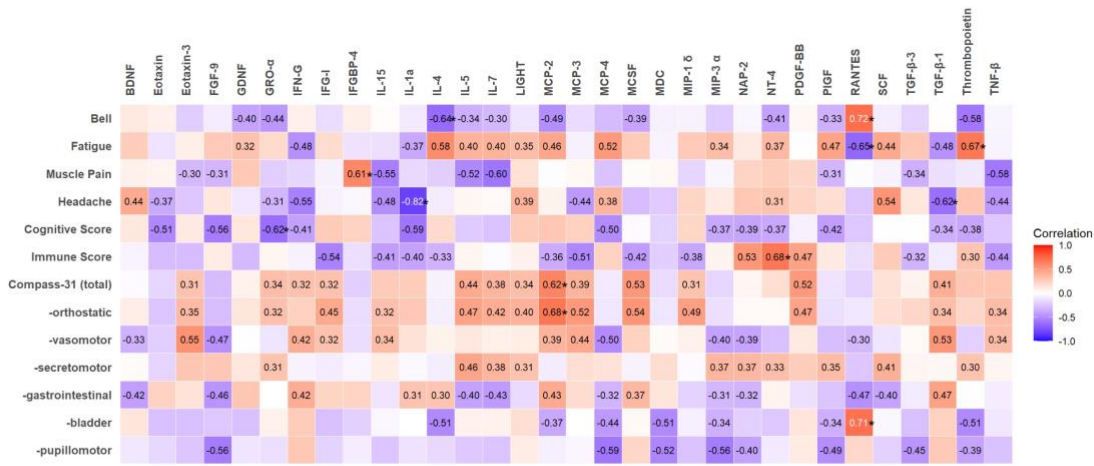
651

Figure 4

A nPCS Cytokine Correlations with Clinical Scores



B pcMECFS Cytokine Correlations with Clinical Scores



652

653

654